Charged Substrate and Product Together Contribute Like a Nonreactive Species to the Overall Electrostatic Steering in Diffusion-Reaction Processes

Jingjie Xu,[†] Yan Xie,[‡] Benzhuo Lu,*,[‡] and Linbo Zhang[‡]

[†]School of Mathematical Sciences, University of Science and Technology of China, Hefei, China

[‡]State Key Laboratory of Scientific and Engineering Computing, Academy of Mathematics and Systems Science, Chinese Academy of Sciences, Beijing, China

ABSTRACT: The Debye–Hückel limiting law is used to study the binding kinetics of substrate–enzyme system as well as to estimate the reaction rate of a electrostatically steered diffusion-controlled reaction process. It is based on a linearized Poisson–Boltzmann model and known for its accurate predictions in dilute solutions. However, the substrate and product particles are in nonequilibrium states and are possibly charged, and their contributions to the total electrostatic field cannot be explicitly studied in the Poisson–Boltzmann model. Hence the influences of substrate and product on reaction rate coefficient were not known. In this work, we consider all the charged species, including the charged substrate, product, and mobile salt ions in a Poisson–Nernst–Planck model, and then compare the results with previous work. The results indicate that both the charged substrate and product can significantly influence the reaction rate coefficient with different behaviors under different setups of computational conditions. It is interesting to find that when substrate and product are both considered, under an overall neutral boundary condition for all the bulk charged species, the computed reaction rate kinetics recovers a similar Debye–Hückel limiting law again. This phenomenon implies that the charged product counteracts the influence of charged substrate on reaction rate coefficient. Our analysis discloses the fact that the total charge concentration of substrate and product, though in a nonequilibrium state individually, obeys an equilibrium Boltzmann distribution, and therefore contributes as a normal charged ion species to ionic strength. This explains why the Debye–Hückel limiting law still works in a considerable range of conditions even though the effects of charged substrate and product particles are not specifically and explicitly considered in the theory.
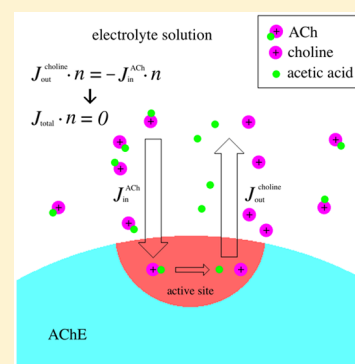
■ INTRODUCTION

The Debye–Hückel limiting law (DHL)[1] is a long established theory for describing the binding kinetics of a substrate–enzyme system, which is also experimentally verified in a range of conditions. The binding rate is a limiting step in diffusion-controlled reaction processes, which also makes DHL applicable to estimate the reaction rate of electrostatically steered diffusion-controlled reactions under different ionic strengths. The Debye–Hückel equation determines the rate coefficient of an acetylcholinesterase (AChE) system as a function of ionic strength I:[2]

$$k_{on} = (k_{on}^0 - k_{on}^H) \times 10^{-1.18|Z_E Z_I|\sqrt{I}} + k_{on}^H \tag{1}$$

Here, the following abbreviations apply: k_{on} is the reaction rate, k_{on}^0 is the effective reaction rate at zero ionic strength rate, k_{on}^H is the effective limiting reaction rate at infinite ionic strength and set to the value of k_{on} calculated at 0.67 M ionic strength, Z_E is the effective enzyme charge, and Z_I is the effective substrate charge. The Debye–Hückel theory is based on the linearized Poisson–Boltzmann (PB) model which is a simplified model of electrolyte solution; nevertheless, the DHL theory enables one to make an accurate prediction which matches well with experimental data.

Usually, ionic strength is measured through bulk concentrations of "spectator" ions (nonreactive mobile ions like Na^+ and Cl^-). However, an issue is raised here that the concentrations of charged substrate and product molecules would also influence the electric field and the reaction rate. Furthermore, the distributions of the reaction-related species are not in an equilibrium state. In this work, we try to properly evaluate the effects of the charged substrate and product to the reaction rate, which are not treated explicitly by the DHL, with a continuum electrodiffusion model. A typical example chosen here is the hydrolysis reaction of acetylcholine (ACh) by AChE[2] (see eq 2). Known as an important enzyme for signal transduction, AChE is tethered to a postsynaptic membrane in neuromuscular junctions, serving to terminate synaptic transmission by hydrolyzing acetylcholine and some other choline esters. Hydrolysis takes place on the active site of AChE, where acetylcholine is catalyzed to acetic acid and choline. As the AChE system is widely studied in biophysics and biochemistry,
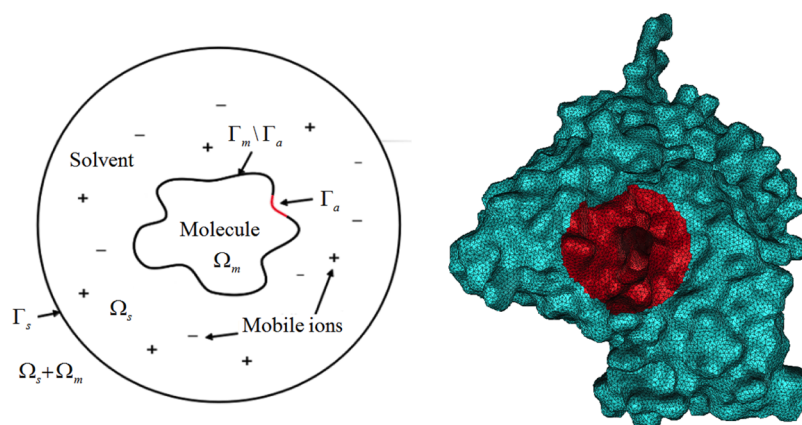
Figure 1. Two-dimensional illustration of computational model and a surface mesh of AChE (from ref 20). The reactive site (boundary) Γ_a is marked in red.

the structure and mechanism of the action of AChE have been elucidated, which facilitates theoretical modeling and numerical simulation. In addition, the impact of electrostatic steering and complex geometry in a diffusion-reaction process is also studied previously by numerical simulations in detail. The chemical reaction equation is as follows:
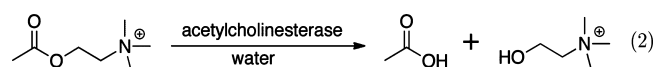
The hydrolysis procedure involves not only intake of ACh but also generation of acetic acid and choline from the active site. It is worth noting that both acetylcholine and choline are positively charged and thus influence the electrostatic field around AChE, while acetic acid is not considered in the current model for its charge neutrality.

The DHL considers the kinetic motion of a charged substrate particle subjected to a background PB electric field. A continuum description of the charge motion under an external electric field usually adopts the drift-diffusion model governed by the Smoluchowski equation[3] or similarly the Nernst–Planck (NP) equations. Earlier NP modeling was used in the theory of electrophoresis of highly charged particles.[4,5] These studies explore the nonequilibrium but steady-state perturbation of a constant external field on the charge distribution around a host ion to see how the host ion is being influenced. It shows that charge polarization effects only become important if the host particle is highly charged. The phenomena studied in the present work are more complicated since we deal with the influence of a spatially varying perturbing field (produced by other charged particles) rather than an external electric field. When an external field is determined by the Poisson–Boltzmann equation,[6–9] the model is the so-called Smoluchowski–Poisson–Boltzmann (SPB) model. The NP or SPB was also applied to describe the substrate diffusion.[10–12] McCammon's group used the SPB model and numerical simulation approaches to study the diffusion-reaction processes of a enzyme–substrate molecular system.[13–16] The SPB equations consist of the Smoluchowski equation[3] and the PB equation. In numerical calculations, the potential field is initially calculated by solving the PB equation. The substrate diffusional flux (drifted by the precalculated PB electric field) is computed by solving the Smoluchowski equation, and the reaction rate is defined as the integration of flux on active site. In the SPB model, the electric field determined by the equilibrium PB equation neglects the contribution from the nonequilibrium

distributed substrate and product species, which is only reasonable at a lower concentration of reactive species. Nevertheless, the numerical results calculated from SPB model seem to fit the DHL law quite well. A proper explanation will be given in this work.

As aforementioned, charged substrate and product molecules are also expected to impose an influence on the reaction, but few studies were made to give a direct and clarified answer to this issue. To consider all the charged particles together, and also notice that the substrate and product are not in an equilibrium state due to reaction, a proper improved approach is to adopt the Poisson–Nernst–Planck equation (PNP)[15,17–21] to simulate the whole electrodiffusion process. The PNP equations consist of a Poisson equation describing the electrostatic field with arbitrary charge distribution (including the transient substrate and product distributions) and Nernst–Planck (NP) equations describing the drift-diffusion of charged particles. The PNP equations are also used in various other studies like diffusions on charged interfaces,[11] and ion transport through an ion channel.[22–24] In the PNP model, the Poisson equation is fully coupled with the NP equation, while the SPB equations are partially coupled. Previous studies show that the uncoupled PB theory may be challenged in estimating the electrostatic potential energy in ion channels.[25–27] The simulations in our previous work using the coupled PNP model show that the reaction rate coefficient is significantly influenced by charged substrate concentration and deviates significantly from the DHL, with different behaviors under different setups of computational conditions.[20,21] In this paper, our PNP model simulates all the charged species together (see Figure 2 in the following section), including charged substrate, product, and mobile ions, and the results are compared with previous work and DHL.

For convenience, we use "PNP1" to indicate the PNP model including substrate species (without the product species) and "PNP2" to indicate the PNP model including both substrate and product species. The models and numerical methods are presented in the next section, and simulation results are compared and discussed in the Numerical Results and Discussions section.

■ METHOD

A solvated biomolecular system is represented in Figure 1, with an illustration of the whole simulation domain Ω on the left and an AChE surface mesh on the right. Mobile ions

("spectator" ions which usually account for ionic strength as a measure of the degree of electrostatic screening) are assumed to distribute continuously in the solvent region and are not able to diffuse across the boundary of biomolecule into the solute region. The solute (molecule) region is represented by Ω_m and the solvent region by Ω_s. Γ_s is the outer boundary, and Γ_m is the boundary of the biomolecule; $\Gamma_a \subset \Gamma_m$ represents the active site in the reaction-diffusion model,[13] which is a 20 Å deep gorge.

Three simulation models are considered in this paper. The first model is the steady-state Smoluchowski–Poisson–Boltzmann equations:[13,14]

$$\nabla \cdot (D_s e^{-\beta q_s \phi(x)} \nabla(c_s(x) e^{\beta q_s \phi(x)})) = 0 \text{ in } \Omega_s \tag{3}$$

$$-\nabla \cdot \epsilon(x) \nabla \phi(x) = \rho^f(x) + \lambda \sum_i q_i c_i^{bulk} e^{-\beta q_i \phi(x)} \text{ in } \Omega \tag{4}$$

Here the summation in eq 4 only includes the nonreactive salt ion species obeying Boltzmann distributions.

The second and third models are the Poisson–Nernst–Planck equations without (PNP1 model) or with (PNP2 model) the charged product species. The Poisson–Nernst–Planck equations are given as follows:[15,20,21]

$$\frac{\partial c_i(x)}{\partial t} = -\nabla \cdot J_i = \nabla \cdot D_i(\nabla c_i(x) + \beta q_i c_i(x) \nabla \phi(x)) \text{ in } \Omega_s$$

$$i = 1, 2, \ldots \tag{5}$$

$$-\nabla \cdot \epsilon(x) \nabla \phi(x) = \rho^f(x) + \lambda \sum_i q_i c_i(x) \text{ in } \Omega \tag{6}$$

where i stands for different species (we only consider at most four charged species, using $i = 1, 2$ to denote the nonreactive salt ions like Na^+ and Cl^-, $i = s$ to denote charged substrate, and $i = p$ to denote charged product). For the ith species, its flux J_i is defined as $-D_i(\nabla c_i(x) + \beta q_i c_i(x) \nabla \phi(x))$, c_i denotes density distribution function, c_i^{bulk} bulk concentration, q_i the charges of each particles, and D_i the diffusion coefficient. ϵ is a piecewise dielectric constant and β the inverse Boltzmann energy. ρ^f denotes the density distribution function of fixed atomic charges in enzyme, λ a characteristic function of Ω_s (1 in Ω_s, and 0 in Ω_m), and ϕ the electrostatic potential function. In this work only the steady state is considered, namely, $\frac{\partial c_i}{\partial t} = 0$. In the PNP1 model only three species, $i = 1, 2, s$, are considered (studied in refs 20 and 21), while in the PNP2 model four species $i = 1, 2, s, p$ are considered.

Dirichlet boundary conditions are used on outer boundary to mimic the bulk situation:

$$\phi = 0, \quad c_i = c_i^{bulk} \quad \text{on } \Gamma_s \tag{7}$$

On Γ_m, boundary conditions differ for different species. In previous work,[13,21] the absorbing boundary condition is set on the reactive boundary for substrate:

$$c_s = 0 \text{ on } \Gamma_a \text{ and } J_s = 0 \text{ on } \Gamma_m \backslash \Gamma_a \tag{8}$$

and nonreactive species have a reflecting boundary on biomolecular boundary:

$$J_i = 0 \text{ on } \Gamma_m \tag{9}$$

In this work, we use a more general and reasonable Robin boundary condition[28,29] at the reactive boundary for substrate species:

$$J_s \cdot n = \alpha c_s \text{ on } \Gamma_a \tag{10}$$

Here α is a reaction coefficient[29] and is set to 10^3 Å^3/μs in our experiments, which can be modified for different kinetics of ligand binding systems and different charged species.

Now, we consider the product species and its boundary condition. According to the chemical reaction in eq 2, every positively charged substrate particle participating in a reaction will finally produce a positively charged product particle (and a neutral product particle, but the neutral species is not considered in this work as it has no influence on the reaction rate within this model). Therefore, the "output" flux of charged product should be equal to the "input" substrate flux, but with opposite direction at the reactive boundary. This is a key point of the current work, and the whole picture is schematically illustrated in Figure 2.
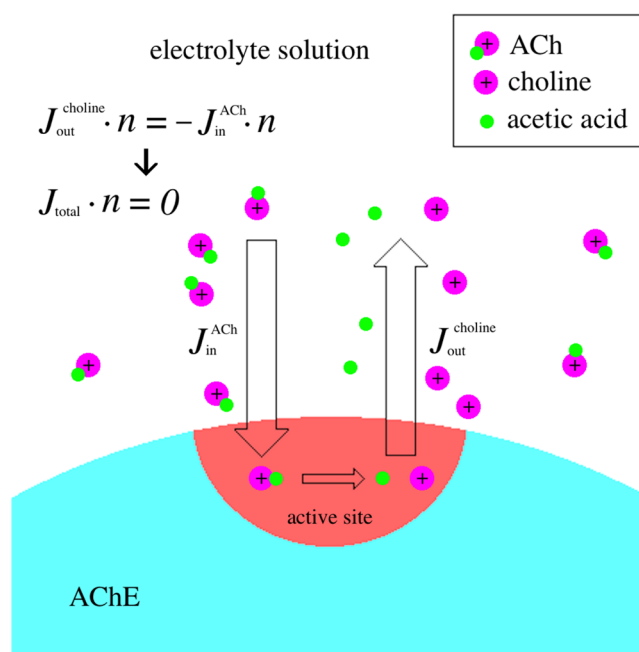
Figure 2. Schematic show of the diffusion-reaction model and the boundary condition for product species in this work.

The above consideration leads to another Robin boundary condition for the charged product species:

$$J_p \cdot n = -J_s \cdot n \text{ on } \Gamma_a \tag{11}$$

This boundary condition of charged product species describes a balance of ionic flow for substrate and product. From eqs 10 and 11 an alternative Robin boundary condition for product in the PNP2 model can be applied for convenience:

$$J_p \cdot n = -\alpha c_s \text{ on } \Gamma_a \tag{12}$$

In our numerical experiments, we compared the Robin boundary condition with the absorbing Dirichlet boundary condition, and observed that the reaction rate coefficients only slightly vary with different boundary conditions, provided that the reaction coefficient α is large. The influence of α on rate coefficient will be reported in the next section.

It is found that the setup of boundary conditions for the species' bulk concentrations strongly affects the calculated reaction rate coefficient. In both situations, i.e., (1) only considering the charge neutrality condition for the two salt ion

species, $c_-^{bulk} = c_+^{bulk}$ (for simplicity, + and − denote the positively and negatively charged salt ion species, respectively), and (2) considering the neutrality condition for two ion species and the positively charged substrate ACh, $c_-^{bulk} = c_+^{bulk} + c_s^{bulk}$, the calculated rate coefficients all strongly depend on the substrate bulk concentration, but the two situations differ from each other and can even lead to very different trends. These studies have been reported in previous work.[20,21] The model PNP1 is considered in situation 2, for which we recalculate some data for comparison in the Numerical Results and Discussions section. When the product species is taken into account in this work, a more reasonable neutral condition is to consider all four species, i.e., $c_-^{bulk} = c_+^{bulk} + c_s^{bulk} + c_p^{bulk}$. Dirichlet boundaries with various bulk concentrations for product species are also tested, but the reaction rate coefficient turns out to be almost the same as long as the over neutrality condition is satisfied at the boundary. Therefore, to simplify the outer boundary conditions, zero concentration is set as the boundary condition on Γ_s for the product species in all the following simulations.

The reaction rate is calculated by integrating the flux of substrate on the reactive boundary:

$$v = \int_{\Gamma_a} J_s \cdot n \, dS \tag{13}$$

and the rate coefficient is the ratio of the reaction rate to the bulk substrate concentration:

$$k = \frac{v}{c_s^{bulk}} \tag{14}$$

where c_s^{bulk} denotes the bulk substrate concentration.

A parallel finite element method is used as our numerical approach, and a body-fitted mesh is adopted, which enables convenient implementation of the above various boundary/interface conditions.[13,24,29]

NUMERICAL RESULTS AND DISCUSSIONS

The implementation of the finite element algorithm is based on the package PHG,[30] and all the calculations were carried out on the cluster LSSC-III of the State Key Laboratory of Scientific and Engineering Computing of Chinese Academy of Sciences.

Before comparing the three models in AChE system, namely, the SPB model, the PNP1 model, and the PNP2 model, we recalculated the numerical results with the PNP1 model[21] as shown in Figure 3, assuming that the diffusion coefficient for ACh is 78 000 Å^2/μs. It is observed that the behaviors of the reaction rate coefficient strongly depend on both substrate concentration and ionic strength, as was discussed in earlier work.[21]

To make more convenient comparisons, in the following analysis, we define "substrate ratio" as the ratio of the bulk substrate concentration to the ionic strength. Actually, in our case the ionic strength is equal to the bulk positive ion concentration in a neutral system (assuming all the charged particle is monovalent), and thus, the substrate ratio equivalently describes the substrate concentration in proportion to the overall positive charge concentration in bulk. In Figure 4, the reaction rate coefficient is represented as a decreasing function of I (ranging from 0 to 0.5 M) with prescribed substrate ratios for both PNP models, while the rate coefficient calculated by the SPB model is not related to the substrate ratio. We calculated the reaction rate coefficient of the PNP1 model with three different ratios, and it is shown that the
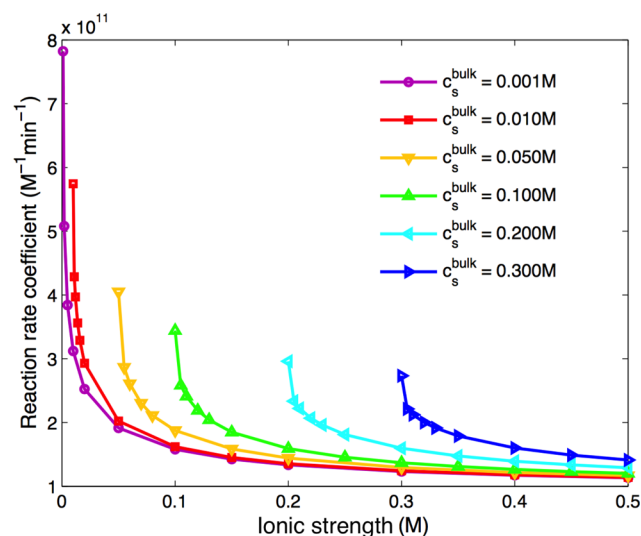
Figure 3. Reaction rate coefficient influenced by ionic strength and substrate concentration in the PNP1 model. x-axis is ionic strength (M), and y-axis is reaction rate coefficient (M^{-1} min^{-1}).
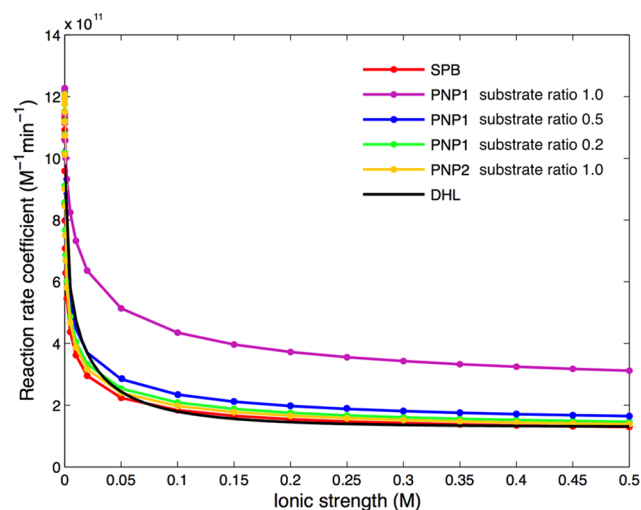
Figure 4. Reaction rate coefficients calculated in SPB, PNP1, and PNP2 models.

reaction rate coefficient increases as the substrate ratio increases. In the PNP2 model, the diffusion coefficient for choline D_p is assumed to be the same as that for ACh (the result dependence on different D_p is shown in Figure 5). It is observed that the reaction rate coefficient is hardly influenced by the substrate ratio in the PNP2 model. Therefore, only one line is plotted with the substrate ratio simply set to 1.0 (results with different substrate ratios are shown in Figure 5). In the ACh−AChE reaction system, the coefficients in DHL are given as follows, $Z_E = -7.91$, $Z_I = +1$.[2]

Different from the PNP1 model, with the above settings, the numerical results of the PNP2 model, the SPB model, and DHL are close to each other. All of these results show an exponential decay of the rate coefficient when the ionic strength increases due to an electrostatic screening effect. The reaction rate coefficients calculated by the PNP1 model are always higher, especially when the substrate ratio is close to 1.0. The difference between PNP1 and PNP2 models decreases as the substrate ratio decreases.
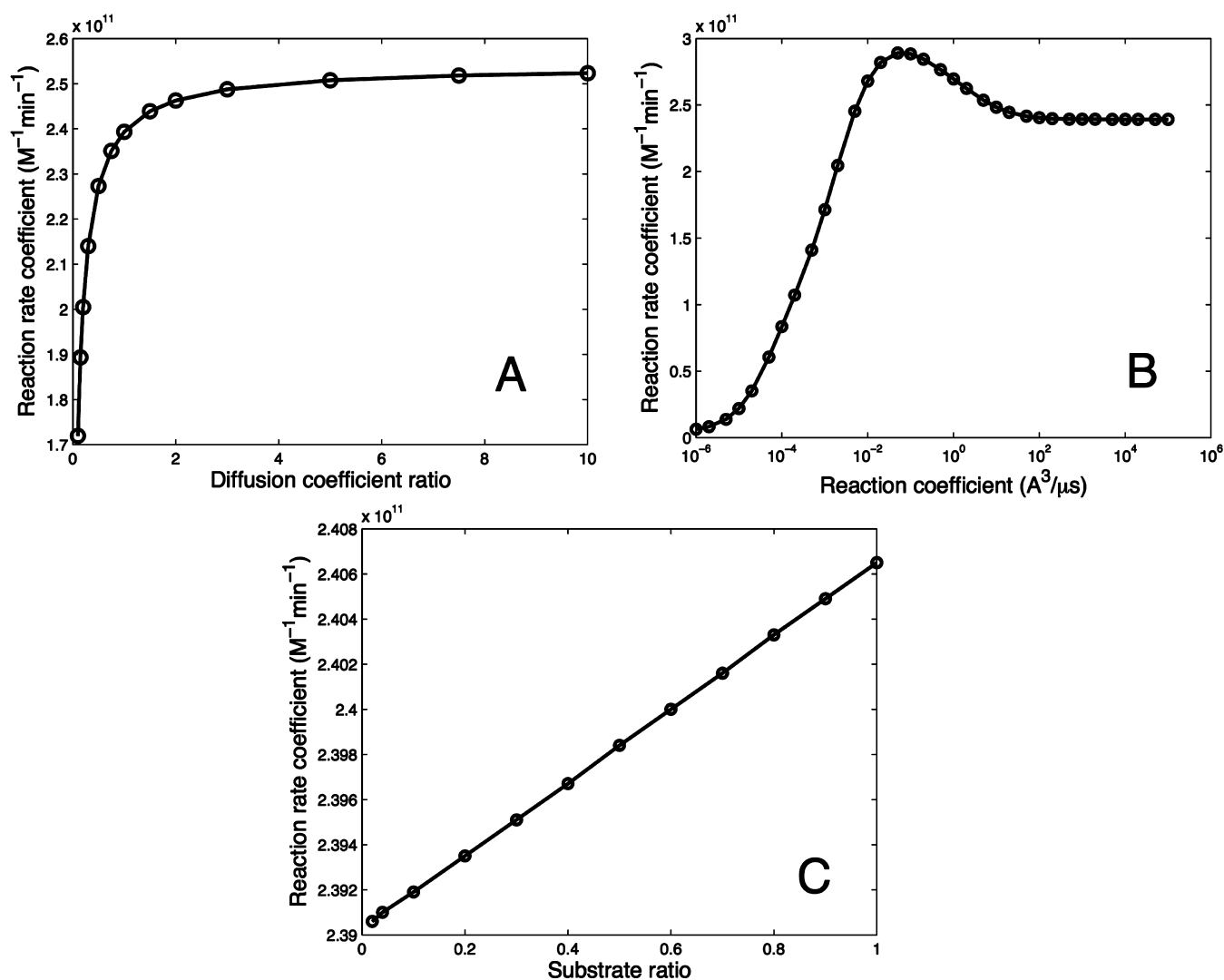
Figure 5. Reaction rate coefficient influenced by (A) diffusion coefficient ratio, (B) reaction coefficient, and (C) substrate ratio in the PNP2 model.

We now try to explain the differences between the three methods. The two PNP models are mainly different in reaction product, as long as the reaction coefficient α is large enough, like $\alpha = 10^3$ Å^3/μs in our simulations. In the PNP2 model, the positively charged choline is assumed to be generated on the biomolecular boundary, where the hydrolyzation takes place and ACh is absorbed. With charged choline considered, more positive charges accumulate around the enzyme in the PNP2 model, producing a stronger ionic screening effect (AChE is overall negatively charged) than in the PNP1 model, and leading to a smaller reaction rate coefficient in the PNP2 model.

A more precise and quantitative explanation for the PNP2 model is as follows. In the simple case that ACh and choline are assumed to have the same diffusion coefficients (like a similar type of particle), the two NP equations for ACh and choline are the same, and their concentrations are additive. This means their total concentration, noted as $c_x = c_s + c_p$, satisfies a similar NP diffusion equation, which can be considered as the concentration of a substitutive imaginary species x with the same positive charge and same diffusion coefficient. Because $J_p \cdot n = -J_s \cdot n$, the imaginary species x has a reflecting boundary condition on the active site Γ_a ($J_{total} \cdot n = J_s \cdot n + J_p \cdot n = 0$, see Figure 2) and a Dirichlet boundary condition on the outer boundary Γ_s. In other words, c_x has a reflective boundary condition on the whole molecular boundary Γ_m. According to the property of PNP equations,[31] if every NP equation satisfies a reflective boundary condition at the molecular boundary and the other conditions are similar to the settings in the PB model, the PNP equations are equivalent to the equilibrium (nonlinear) PB equation, indicating zero fluxes everywhere. This means that c_x and other concentrations of salt ion species obey Boltzmann distributions in AChE system, and the total potential field is the same as a nonlinear PB potential field (note that a similar overall charge neutrality condition also holds at the outer boundary for all the charged species), though each individual of c_s and c_p does not follow a Boltzmann distribution due to their nonequilibrium property (nonzero flux). The physical consequence in this situation is that the substrate ACh is subject to an exact PB potential field during its diffusive binding process and behaves like a field "probing" particle without considering its self-influence to the potential field as in the SPB model. This explains the reason why in Figure 4 our PNP2 model yields very close predictions as in the SPB model, and both PNP2 and SPB models fit the Debye–Hückel limiting law well. A difference is that the PNP2 model inherently coincides with the nonlinear PB model (with certain setup of diffusion coefficients and neutrality condition satisfied

as discussed above), and DHL is based on the linearized PB. In addition, if the substrate and product have quite different diffusion coefficients and/or do not bring similar charge(s), or if the reaction coefficient α is not large enough as shown in Figure 5, the PNP2 model may generate different results from the SPB model and DHL. Both previous SPB model and DHL assume a very fast chemical reaction step (large α). However, according to above observations and physical explanations, the PNP2 model seems to be applicable in more general situations.

In Figure 5, we show how different coefficients, including product/substrate diffusion coefficients, reaction coefficient, and substrate ratio, influence the reaction rate coefficient in the new PNP2 model. The condition and coefficients in Figure 5 are given as follows for each subfigure if not specified: $I = 0.5$ M, substrate ratio = 0.2, diffusion coefficient ratio = 1, reaction coefficient = 10^3 Å$^3/\mu$s. The "diffusion coefficient ratio" is defined as the ratio of choline diffusion coefficient D_p to ACh diffusion coefficient D_s. As shown in Figure 5A, the diffusion coefficient ratio strongly influences the reaction rate coefficient. We consider two kinds of extreme situations: one is that the diffusion coefficient ratio is very small, so that choline accumulates around the active site, which hinders the reaction process and reduces the reaction rate coefficient; the other one is that if the diffusion coefficient ratio is large enough, the choline would diffuse quickly, and the accumulation effect disappears and approaches the limiting case. In fact, the choline molecule is smaller in size than ACh. From the Stokes–Einstein relation, D_p can be estimated to be slightly larger than D_s, so a reasonable diffusion coefficient ratio for choline and ACh system should be a little bit larger than 1. Figure 5B shows how the reaction coefficient influences the results. At small reaction coefficient, the reaction rate coefficient is small because the reaction is slowed by the chemical reaction step. When the reaction coefficient α becomes large enough, diffusion is the limiting step for the overall reaction process and the reaction rate coefficient is completely diffusion-controlled, in which case the rate coefficient approaches its diffusion rate limit. Two extreme cases are $\alpha = 0$ (representing nonreaction) and $\alpha = +\infty$ (representing the "perfect" reaction). However, we have no good reason to explain why there is an extreme point at about $\alpha = 10^{-1}$ Å$^3/\mu$s. It is found in Figure 5C that an increase in substrate ratio can very slightly increase the rate coefficient, but the influence is only within 1% of the overall magnitude. This is why we only use the data from the substrate ratio equal to 1.0 in Figure 4.

CONCLUSIONS

A comparative study is done for three numerical models and the DHL for estimation of the reaction rate coefficient of the diffusion-controlled reaction system ACh-AChE. The following conclusions can be drawn through the results and analysis: (1) All the charged species including salt ions, charged substrate, and product (if not negligibly dilute) play significant roles in influencing the reaction rate coefficient, and both the charged substrate and product contribute to electrostatic screening which is similar to the ionic strength in DHL. (2) Boundary conditions, especially the method for setting up the neutrality condition, can also strongly influence the calculated results. (3) The Debye–Hückel limiting law describes well the electrostatic steering effects in diffusion-reaction processes for a range of conditions without the need to specifically consider the influence of the charged substrate and product on the overall electric field. The model PNP2, considering the electric field

from all the charged species, especially including the substrate and product, yields very close results to those of SPB and DHL for a range of conditions (provided that the overall neutrality condition at outer boundary is satisfied), whereas the SPB model and DHL do not explicitly and self-consistently (as the coupled PNP equations) take into account the charge effect of substrate and product in their underlying theory. As explained in the previous section for the PNP2 model, the overall influence of substrate and product is almost like the effect of a single imaginary nonreactive species, indicating that the total charge concentration of substrate and product obeys the Boltzmann distribution and contributes as a component of the overall ionic strength and screening. This means that the simpler models such as DHL and SPB can in fact produce the correct electrostatic interactions in diffusion-reaction processes, and give reasonable predictions for a considerable range of conditions. (4) A model as PNP1 considering the substrate but without the charged product most likely leads to unacceptable results except for in the case with very low substrate bulk concentrations. Although the original goal of the PNP1 model is to improve the SPB model by considering an additional species, the substrate, the results become worse (because the ignored product can actually compensate the substrate in terms of electrostatic screening). (5) The relatively complete model PNP2 considering all the charged species can be in principle applicable to various and more general conditions, such as very low or high diffusion coefficient ratios, low reaction coefficient, or non-neutral conditions if they exist.

When the mean field PNP theory is challenged, other factors such as particle size effects, correlation effects, and molecular flexibility need to be considered beyond the current model.[32−35]

AUTHOR INFORMATION

Corresponding Author

*E-mail: bzlu@lsec.cc.ac.cn. Phone: 086-10-82541904.

Notes

The authors declare no competing financial interest.

REFERENCES

(1) Debye, P.; Hückel, E. Zur Theorie der Elektrolyte. *Phys. Zeitschr.* **1923**, *24*, 185−206.

(2) Radić, Z.; Kirchhoff, P. D.; Quinn, D. M.; McCammon, J. A.; Taylor, P. Electrostatic Influence on the Kinetics of Ligand Binding to Acetylcholinesterase. *J. Biol. Chem.* **1997**, *272*, 23265−23277.

(3) Smoluchowski, M. V. Versuch einer mathematischen Theorie der koagulationskinetik kolloider Lönsungen. *Z. Phys. Chem.* **1917**, *92*, 129−168.

(4) Booth, F. The Cataphoresis of Spherical, Solid Non-Conducting Particles in a Symmetrical Electrolyte. *Proc. R. Soc. London, Ser. A* **1950**, *203*, 514−533.

(5) Wiersema, P. H.; Loeb, A. L.; Overbeek, J. T. G. Calculation of the Electrophoretic Mobility of a Spherical Colloid Particle. *J. Colloid Interface Sci.* **1966**, *22*, 78−99.

(6) Gouy, G. Constitution of the electric charge at the surface of an electrolyte. *J. Phys. Theor. Appl.* **1910**, *9*, 457−468.

(7) Chapman, D. L. A. Contribution to the Theory of Electro-capillarity. *Philos. Mag.* **1913**, *25*, 475−481.

(8) Honig, B.; Nicholls, A. Classical electrostatics in biology and chemistry. *Science* **1995**, *268*, 1144−1149.

(9) Baker, N. A. Poisson-Boltzmann Methods for Biomolecular Electrostatics. *Methods Enzymol.* **2004**, *383*, 94−118.

(10) Cohen, H.; Cooley, J. W. The Numerical Solution of the Time-Dependent Nernst-Planck Equations. *Biophys. J.* **1965**, *5*, 145−162.

(11) Chan, D. Y.; Halle, B. The Smoluchowski-Poisson-Boltzmann Description of Ion Diffusion at Charged Interfaces. *Biophys. J.* **1984**, *46*, 387−407.

(12) Zhou, H. X. Kinetics of Diffusion-Influenced Reactions Studied by Brownian Dynamics. *J. Phys. Chem.* **1990**, *94*, 8794−8800.

(13) Song, Y. H.; Zhang, Y. J.; Shen, T. Y.; Bajaj, C. L.; McCammon, J. A.; Baker, N. A. Finite Element Solution of the Steady-State Smoluchowski Equation for Rate Constant Calculations. *Biophys. J.* **2004**, *86*, 2017−2029.

(14) Zhang, D. Q.; Suen, J. K.; Zhang, Y. J.; Song, Y. H.; Radić, Z.; Taylor, P.; Holst, M. J.; Bajaj, C. L.; Baker, N. A.; McCammon, J. A. Tetrameric Mouse Acetylcholinesterase: Continuum Diffusion Rate Calculations by Solving the Steady-State Smoluchowski Equation Using Finite Element Methods. *Biophys. J.* **2005**, *88*, 1659−1665.

(15) Lu, B. Z.; Zhou, Y. C.; Huber, G. A.; Bond, S. D.; Holst, M. J.; McCammon, J. A. Electrodiffusion: A continuum modeling framework for biomolecular systems with realistic spatiotemporal resolution. *J. Chem. Phys.* **2007**, *127*, 135102.

(16) Cheng, Y. H.; Suen, J. K.; Zhang, D. Q.; Bond, S. D.; Zhang, Y. J.; Song, Y. H.; Baker, N. A.; Bajaj, C. L.; Holst, M. J.; McCammon, J. A. Finite Element Analysis of the Time-Dependent Smoluchowski Equation for Acetylcholinesterase Reaction Rate Calculations. *Biophys. J.* **2007**, *92*, 3397−3406.

(17) Eisenberg, R. S. Channels as Enzymes: Oxymoron and Tautology. *J. Membr. Biol.* **1990**, *115*, 1−12.

(18) Eisenberg, R. S. Computing the Field in Proteins and Channels. *J. Membr. Biol.* **1996**, *150*, 1−25.

(19) Barcilon, V.; Chen, D. P.; Eisenberg, R. S.; Jerome, J. W. Qualitative properties of steady-state Poisson-Nernst-Planck systems: Perturbation and simulation study. *SIAM J. Appl. Math.* **1997**, *57*, 631−648.

(20) Zhou, Y. C.; Lu, B. Z.; Huber, G. A.; Holst, M. J.; McCammon, J. A. Continuum Simulations of Acetylcholine Consumption by Acetylcholinesterase: A Poisson-Nernst-Planck Approach. *J. Phys. Chem. B* **2008**, *112*, 270−275.

(21) Lu, B. Z.; McCammon, J. A. Kinetics of diffusion-controlled enzymatic reactions with charged substrates. *PMC Biophys.* **2010**, *3*, 1.

(22) Nonner, W.; Eisenberg, B. Ion Permeation and Glutamate Residues Linked by Poisson-Nernst-Planck Theory in L-Type Calcium Channels. *Biophys. J.* **1998**, *75*, 1287−1305.

(23) Kurnikova, M. G.; Coalson, R. D.; Graf, P.; Nitzan, A. A Lattice Relaxation Algorithm for Three-Dimensional Poisson-Nernst-Planck Theory with Application to Ion Transport through the Gramicidin A Channel. *Biophys. J.* **1999**, *76*, 642−656.

(24) Tu, B.; Chen, M. X.; Xie, Y.; Zhang, L. B.; Eisenberg, B.; Lu, B. Z. A Parallel Finite Element Simulator for Ion Transport through Three-Dimensional Ion Channel Systems. *J. Comput. Chem.* **2013**, *34*, 2065−2078.

(25) Moy, G.; Corry, B.; Kuyucak, S.; Chung, S. H. Tests of Continuum Theories as Models of Ion Channels. I. Poisson-Boltzmann Theory versus Brownian Dynamics. *Biophys. J.* **2000**, *78*, 2349−2363.

(26) Corry, B.; Kuyucak, S.; Chung, S. H. Tests of Continuum Theories as Models of Ion Channels. II. Poisson-Nernst-Planck Theory versus Brownian Dynamics. *Biophys. J.* **2000**, *78*, 2364−2381.

(27) Im, W.; Roux, B. Ions and Counterions in a Biological Channel: A Molecular Dynamics Simulation of OmpF Porin from *Escherichia coli* in an Explicit Membrane with 1 M KCl Aqueous Salt Solution. *J. Mol. Biol.* **2002**, *319*, 1177−1197.

(28) Ryan, E. M.; Tartakovsky, A. M.; Amon, C. A novel method for modeling Neumann and Robin boundary conditions in smoothed

particle hydrodynamics. *Comput. Phys. Commun.* **2010**, *181*, 2008−2023.

(29) Pan, W. X.; Daily, M.; Baker, N. A. Numerical calculation of protein-ligand binding rates through solution of the Smoluchowski equation using smoothed particle hydrodynamics. *BMC Biophys.* **2015**, *8*, 7.

(30) Zhang, L. B. A. Parallel Algorithm for Adaptive Local Refinement of Tetrahedral Meshes Using Bisection. *Numer. Math. Theor. Meth. Appl.* **2009**, *2*, 65−89.

(31) Lu, B. Z.; Zhou, Y. C. Poisson-Nernst-Planck Equations for Simulating Biomolecular Diffusion-Reaction Processes II: Size Effects on Ionic Distributions and Diffusion-Reaction Rates. *Biophys. J.* **2011**, *100*, 2475−2485.

(32) Roth, R.; Gillespie, D. Physics of Size Selectivity. *Phys. Rev. Lett.* **2005**, *95*, 247801.

(33) Boda, D.; Nonner, W.; Valiskó, M.; Henderson, D.; Eisenberg, B.; Gillespie, D. Steric Selectivity in Na Channels Arising from Protein Polarization and Mobile Side Chains. *Biophys. J.* **2007**, *93*, 1960−1980.

(34) Zhou, H. X.; Wlodek, S. T.; McCammon, J. A. Conformation Gating as a Mechanism for Enzyme Specificity. *Proc. Natl. Acad. Sci. U. S. A.* **1998**, *95*, 9280−9283.

(35) Beri, V.; Auletta, J. T.; Maharvi, G. M.; Wood, J. F.; Fauq, A. H.; Rosenberry, T. L. Hydrolysis of low concentrations of the acetylthiocholine analogs acetyl(*homo*)thiocholine and acetyl(*nor*)-thiocholine by acetylcholinesterase may be limited by selective gating at the enzyme peripheral site. *Chem.-Biol. Interact.* **2013**, *203*, 38−43.